Supplementary Material: Generalized Content-Preserving Warps for Image Stitching

This supplementary document consists of three parts. The first part presents the datasets that we use in our experiments. The second part describes the detailed generation process of synthetic images with different degrees of colour variation, which is related to the Section 3.1 of the paper. The third part provides more comparative results with higher image resolution.

1 Datasets

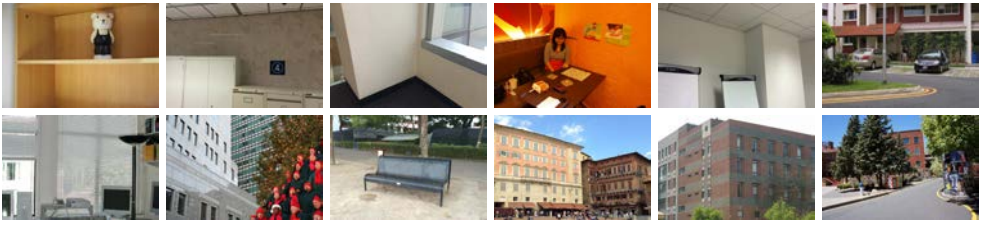

Figure 1: Dataset1 consists of 12 pairs of images. First row: pair 01-06. Second row: pair 07-12. Each pair of images has nearly no colour differences, which are collected from [1, 2, 4]. Dataset1 is used in our synthetic experiments (Section 3.1 of the paper).

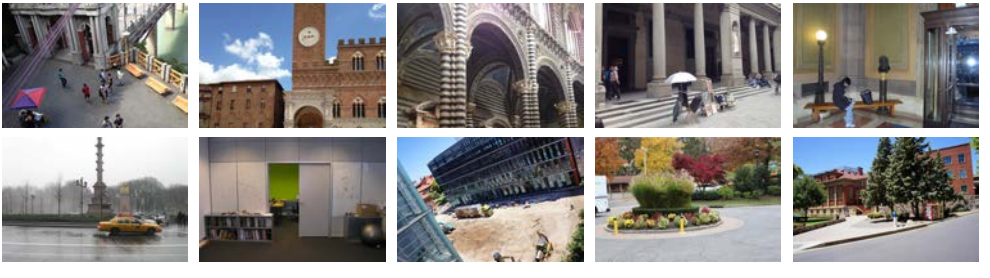

Figure 2: Dataset2 consists of 10 pairs of images. First row: pair 01-05. Second row: pair 06-10. Each pair of images has significant colour differences and are directly collected from [1, 2, 4]. We use Dataset2 to conduct our experiments on real images (Section 3.2 of the paper).

2 Generating Images with Colour Variation

As described in the paper, for each pair of images in the Dataset1, we generate N pairs of images ($N = 16$ in our implementation) with different degrees of colour variations to obtain

our synthetic data. In order to control the degree of colour variation, we adopt the global colour model [3]:

$$I' = (cI)^{\gamma}, \tag{1}$$

where I is the original image, I' is the synthetic image, c is a scale factor that is related to the white balance ($c = 1.0$ in our implementation) and $(.)^{\gamma}$ is the non-linear gamma function. In order to create more complex variation that is relevant to spatial positions, we add a spatially-varying factor to the non-linear gamma function and compute the γ of Eq.1 as follows:

$$\gamma = (1 + \frac{k-1}{N})^{-a/b} \times \beta, \tag{2}$$

where $k = 1, 2, 3, ..., N$ denotes the pair index, a is the pixel column coordinate (or row coordinate), b is the image width (or image height). With Eq. 2, we use different values of γ for pixels located on different positions to simulate the local colour variation. We synthesis the colour difference from small to large (k varies from 1 to N) according to the colour model defined by Eq. 1. Specifically, we first convert the source image from *RGB* colour space to *YCbCr* colour space. We then conduct colour transformation for each image channel independently. For image Y-channel, we sample the value of β from 1.0 to 0.5. For other two image channels, we sample β from 1.0 to 0.95. Figure 3 presents one group of our synthetic images.

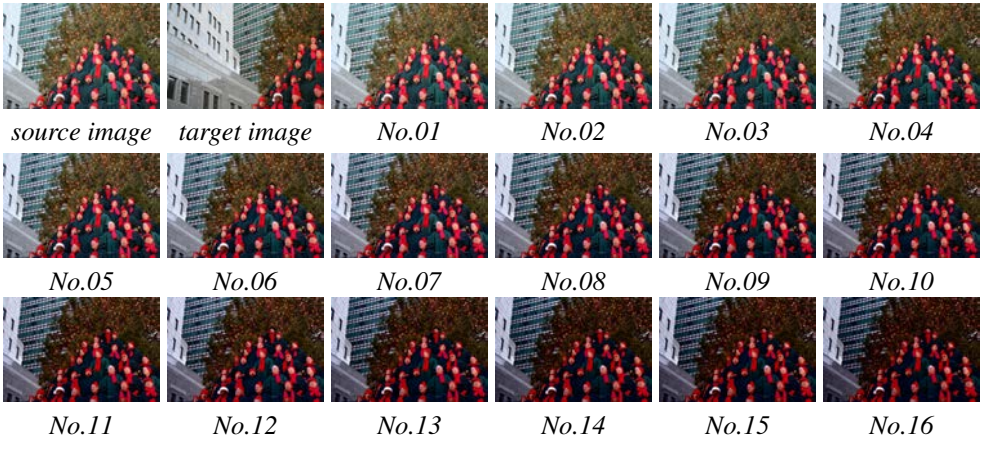

Figure 3: One group of synthetic images generated with our scheme. It consists of 16 pairs of images. We control the colour differences from small to large.

3 Comparative Results

In this part, we present more comparative results with higher image resolution. Specifically, Figure 4 to Figure 9 shows our results on all 12 groups of synthetic images of Dataset1. As for experiments on Dataset2, from Figure 10 to Figure 13, we present the results of our method compared with Global Homography, CPW and DF-W. From Figure 14 to Figure 19, we present the detailed results of our method compared with DF-W, MF-W, LSH+MF-W and ROS+MF-W.

References

[1] Yu-Sheng Chen and Yung-Yu Chuang. Natural image stitching with the global similarity prior. In *European Conference on Computer Vision (ECCV)*, pages 186–201, 2016.

[2] Shiwei Li, Lu Yuan, Jian Sun, and Long Quan. Dual-feature warping-based motion model estimation. In *IEEE International Conference on Computer Vision (ICCV)*, pages 4283–4291, 2015.

[3] Jaesik Park, Yu-Wing Tai, Sudipta N Sinha, and In So Kweon. Efficient and robust color consistency for community photo collections. In *IEEE Conference on Computer Vision and Pattern Recognition (CVPR)*, pages 430–438, 2016.

[4] Julio Zaragoza, Tat-Jun Chin, Michael S Brown, and David Suter. As-projective-as-possible image stitching with moving dlt. In *IEEE Conference on Computer Vision and Pattern Recognition (CVPR)*, pages 2339–2346, 2013.

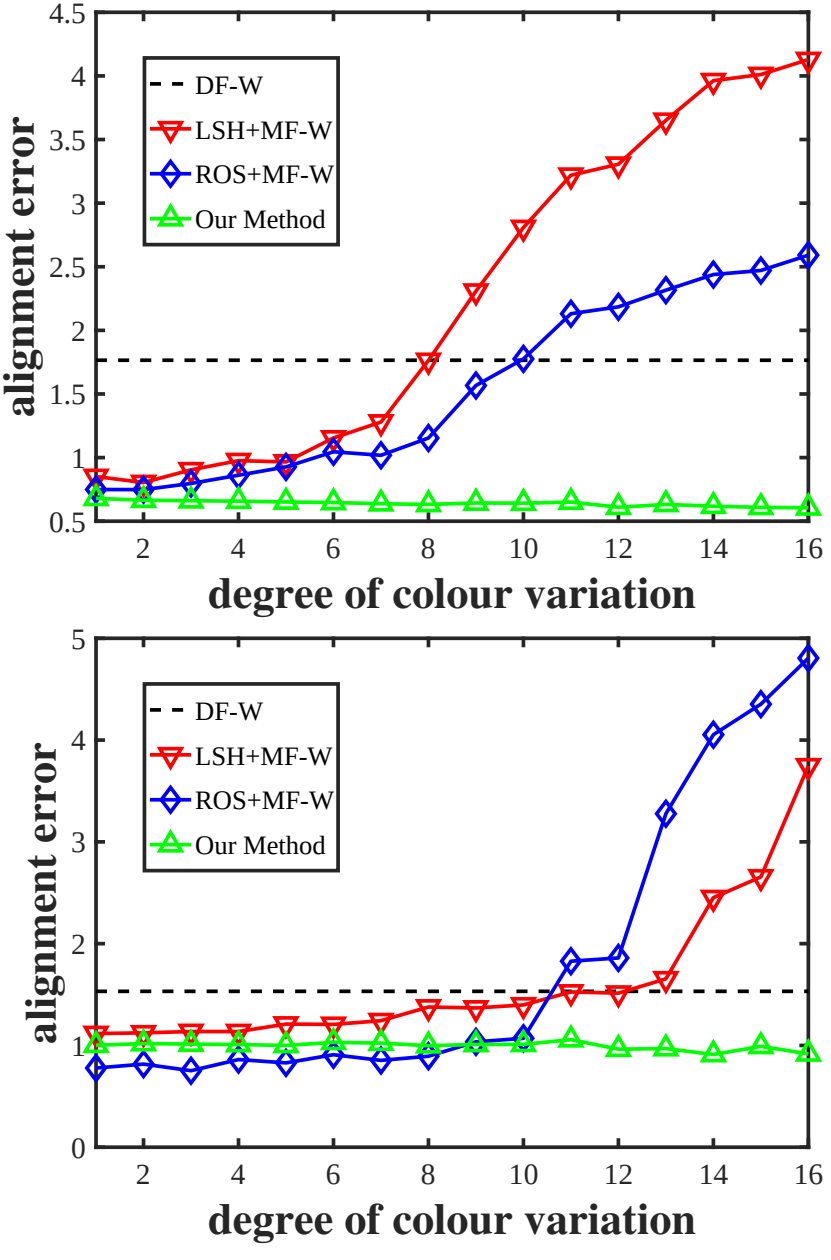

Figure 4: Comparative results on image pair 01-02.

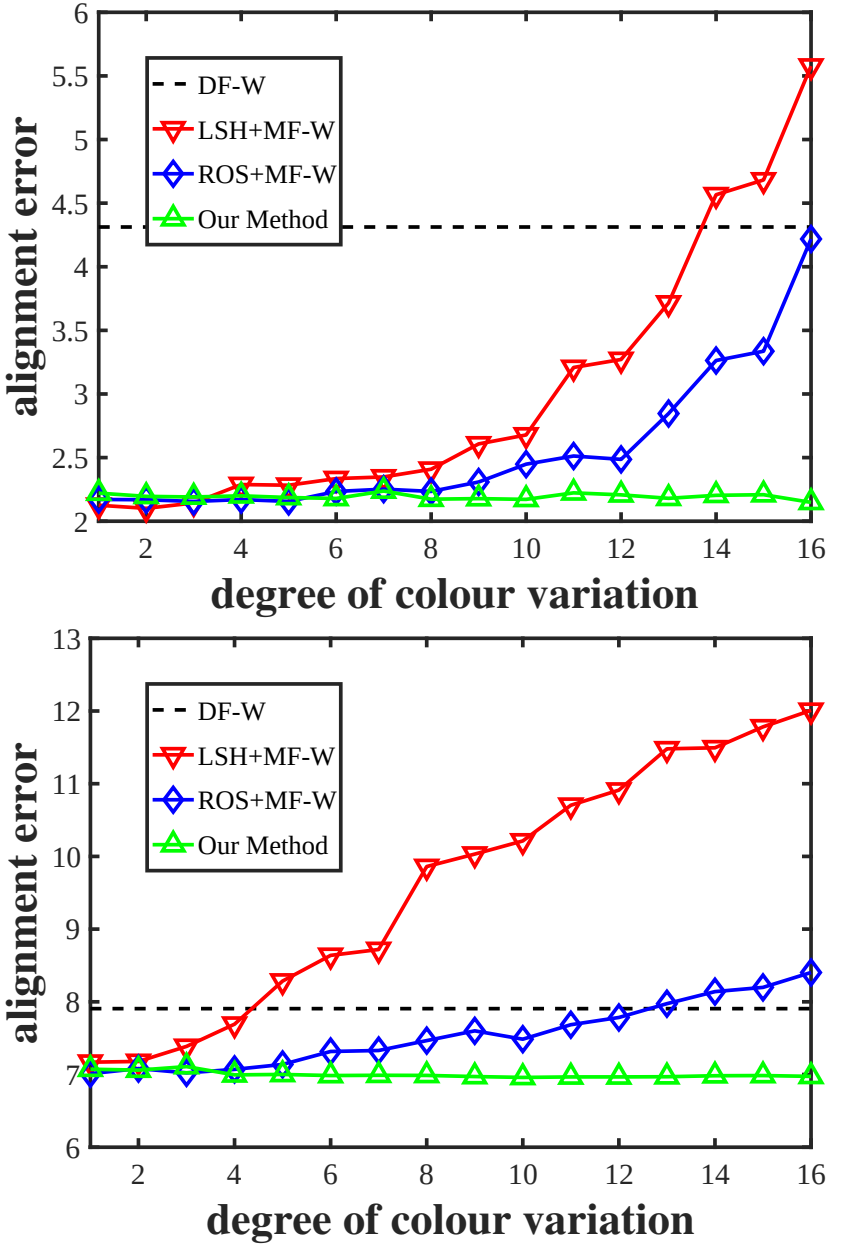

Figure 5: Comparative results on image pair 03-04.

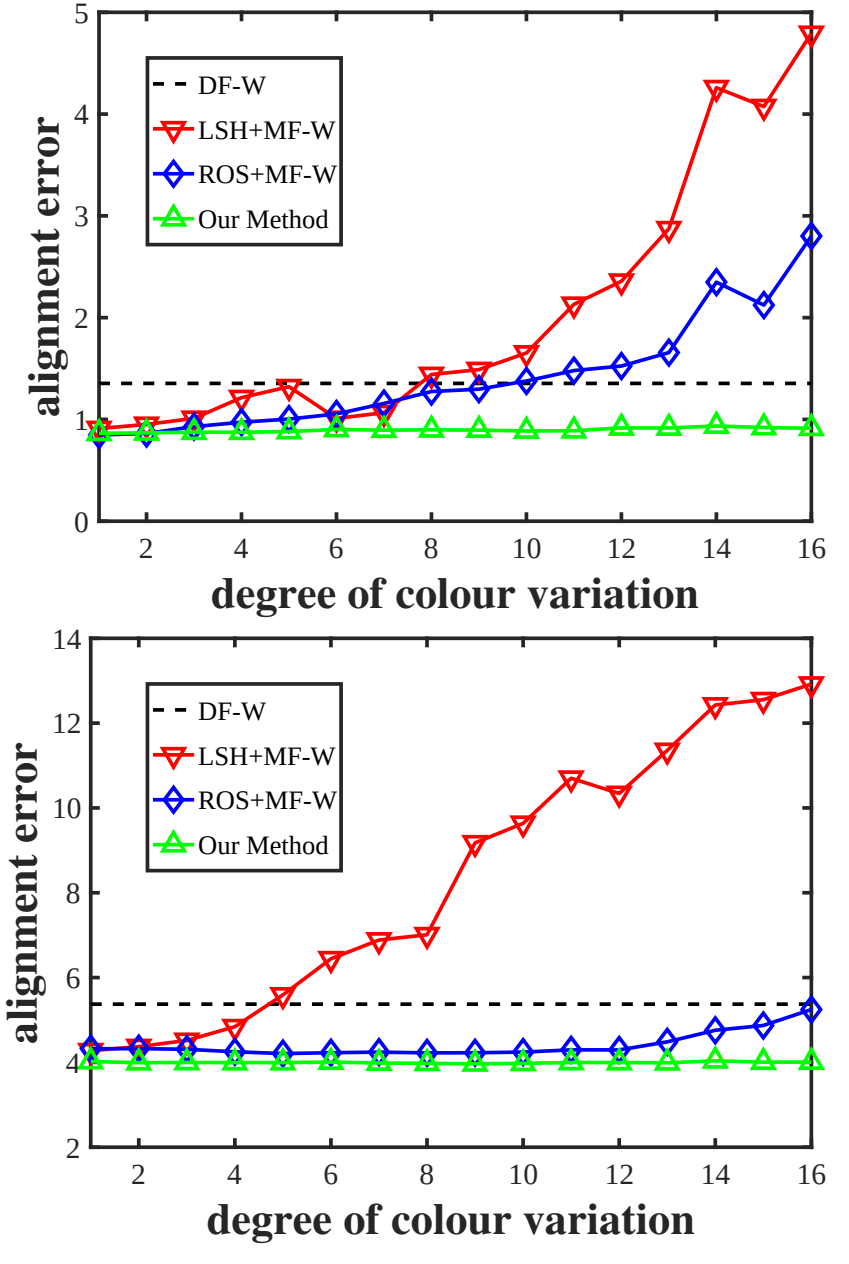

Figure 6: Comparative results on image pair 05-06.

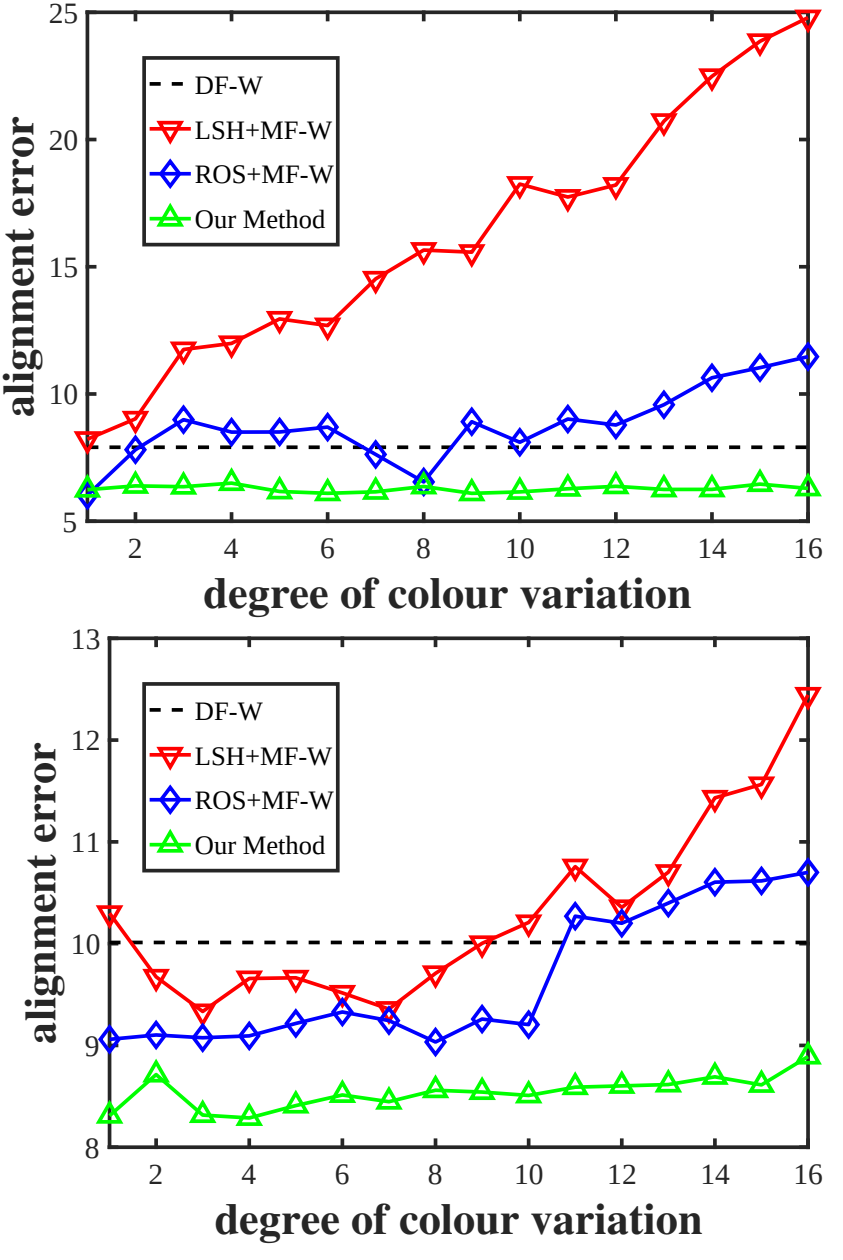

Figure 7: Comparative results on image pair 07-08.

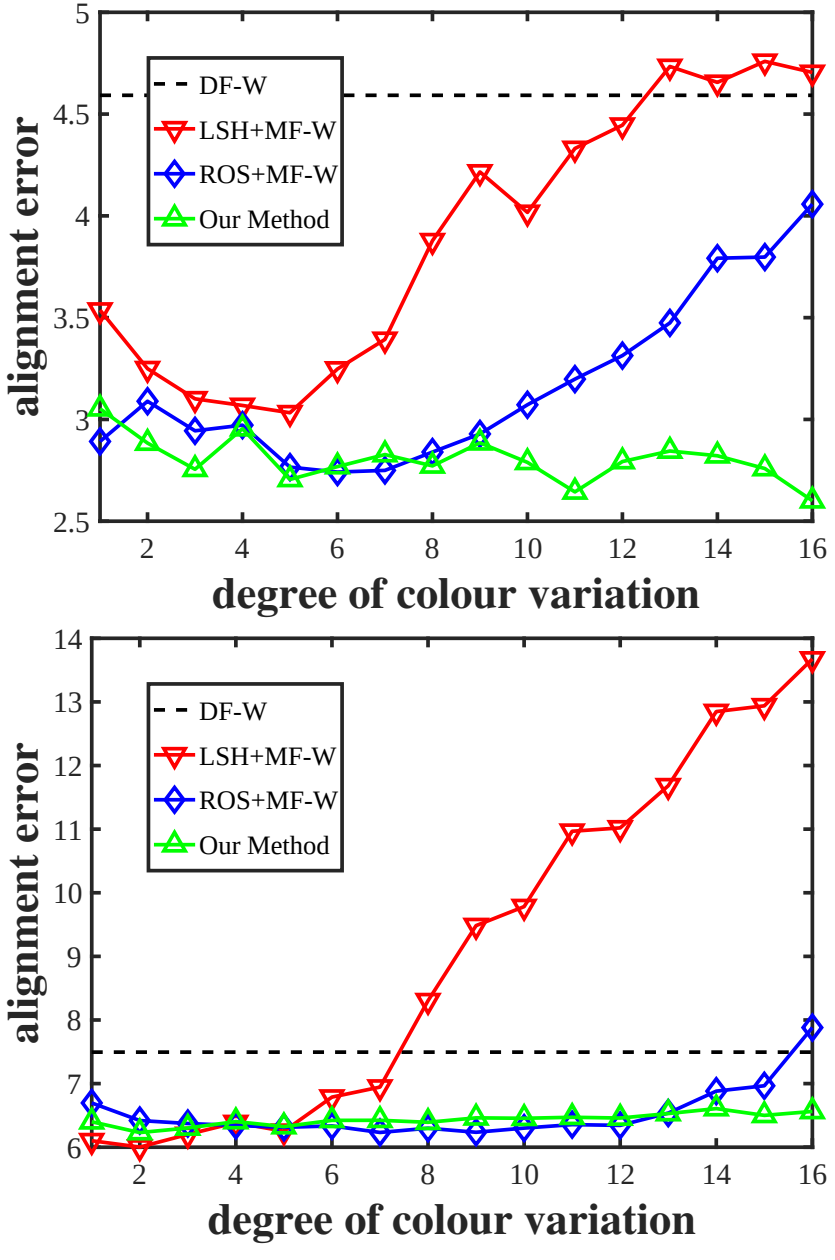

Figure 8: Comparative results on image pair 09-10.

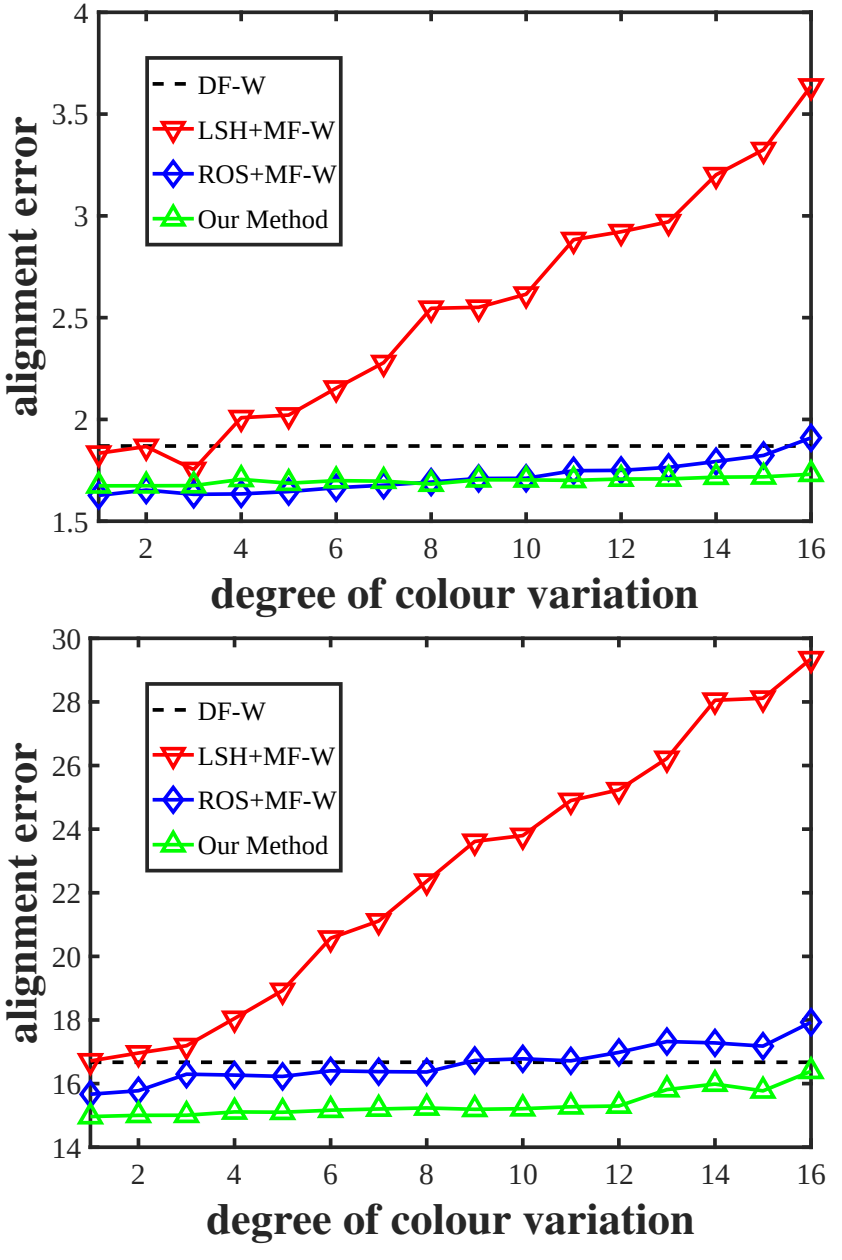

Figure 9: Comparative results on image pair 11-12.

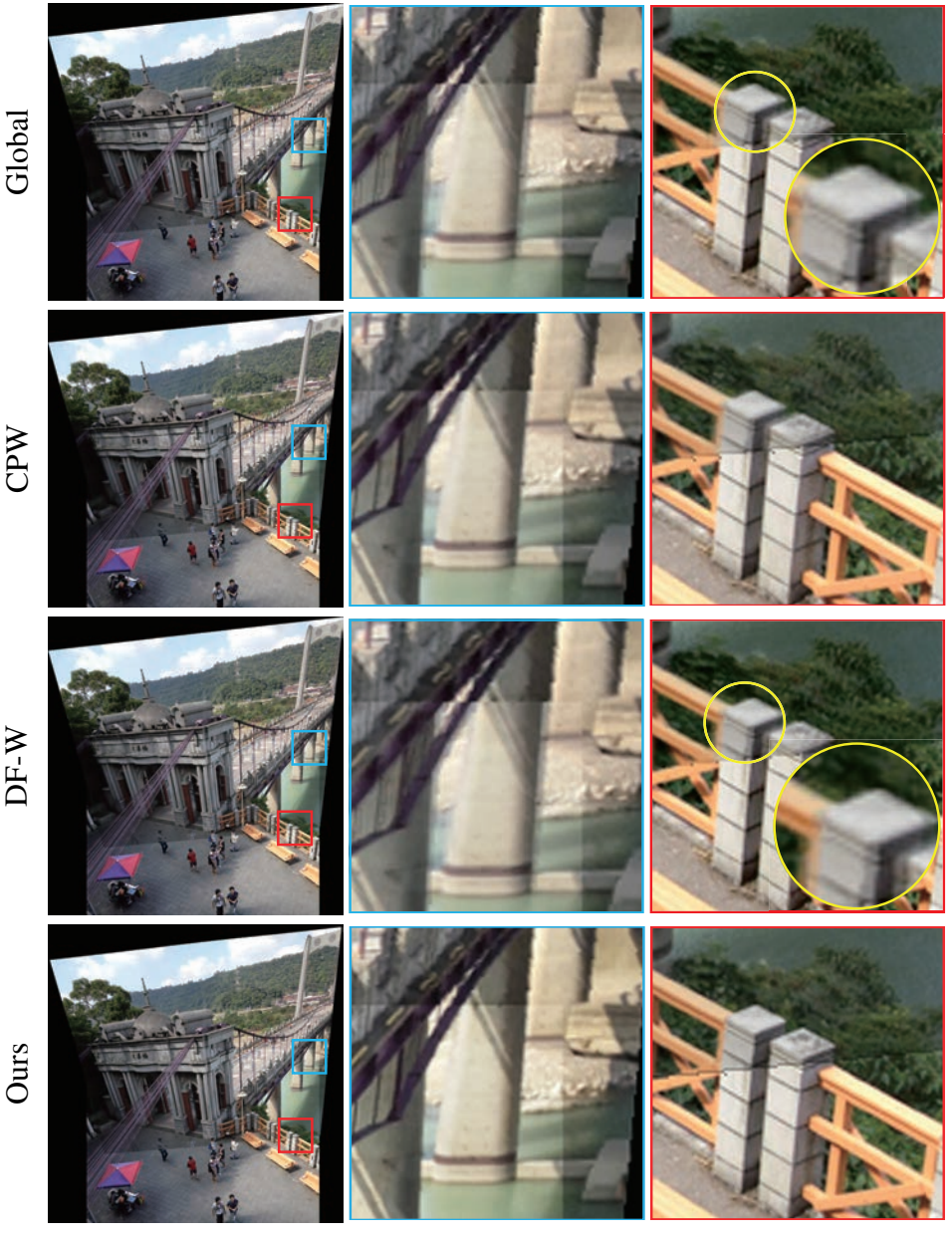

Figure 10: Comparisons with Global Homography, CPW and DF-W: Image pair 01.

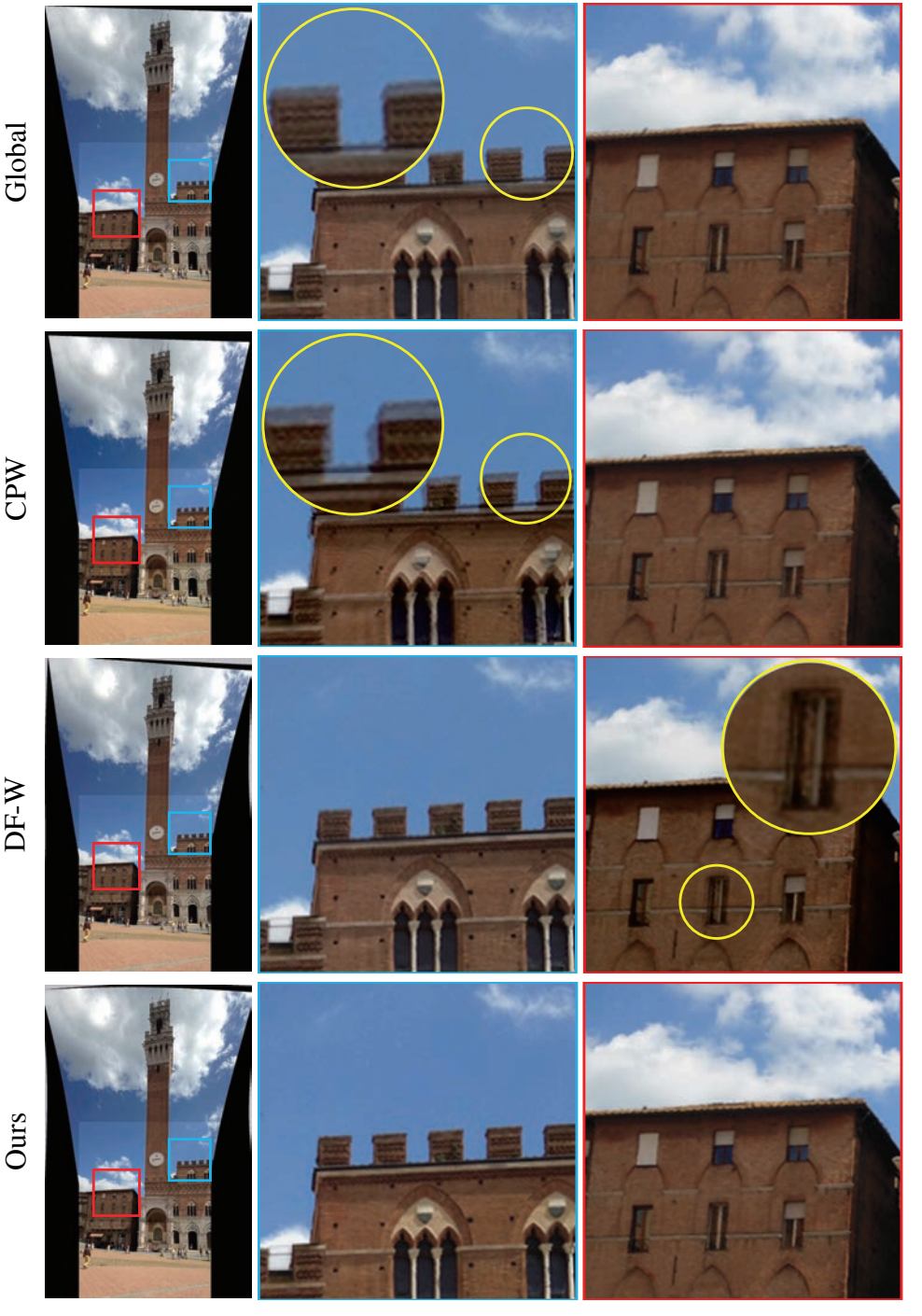

Figure 11: Comparisons with Global Homography, CPW and DF-W: Image pair 02.

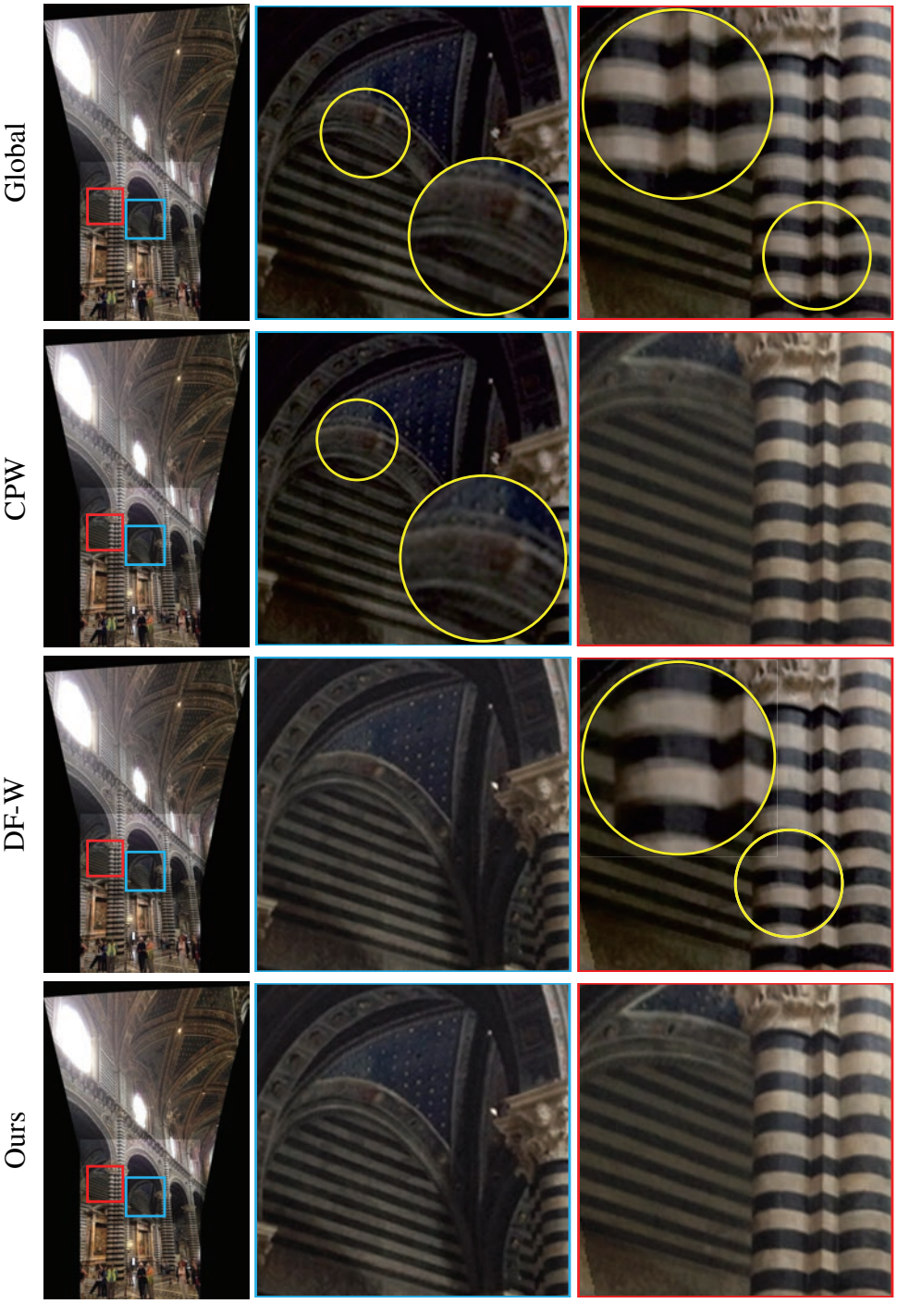

Figure 12: Comparisons with Global Homography, CPW and DF-W: Image pair 03.

Figure 13: Comparisons with Global Homography, CPW and DF-W: Image pair 04.

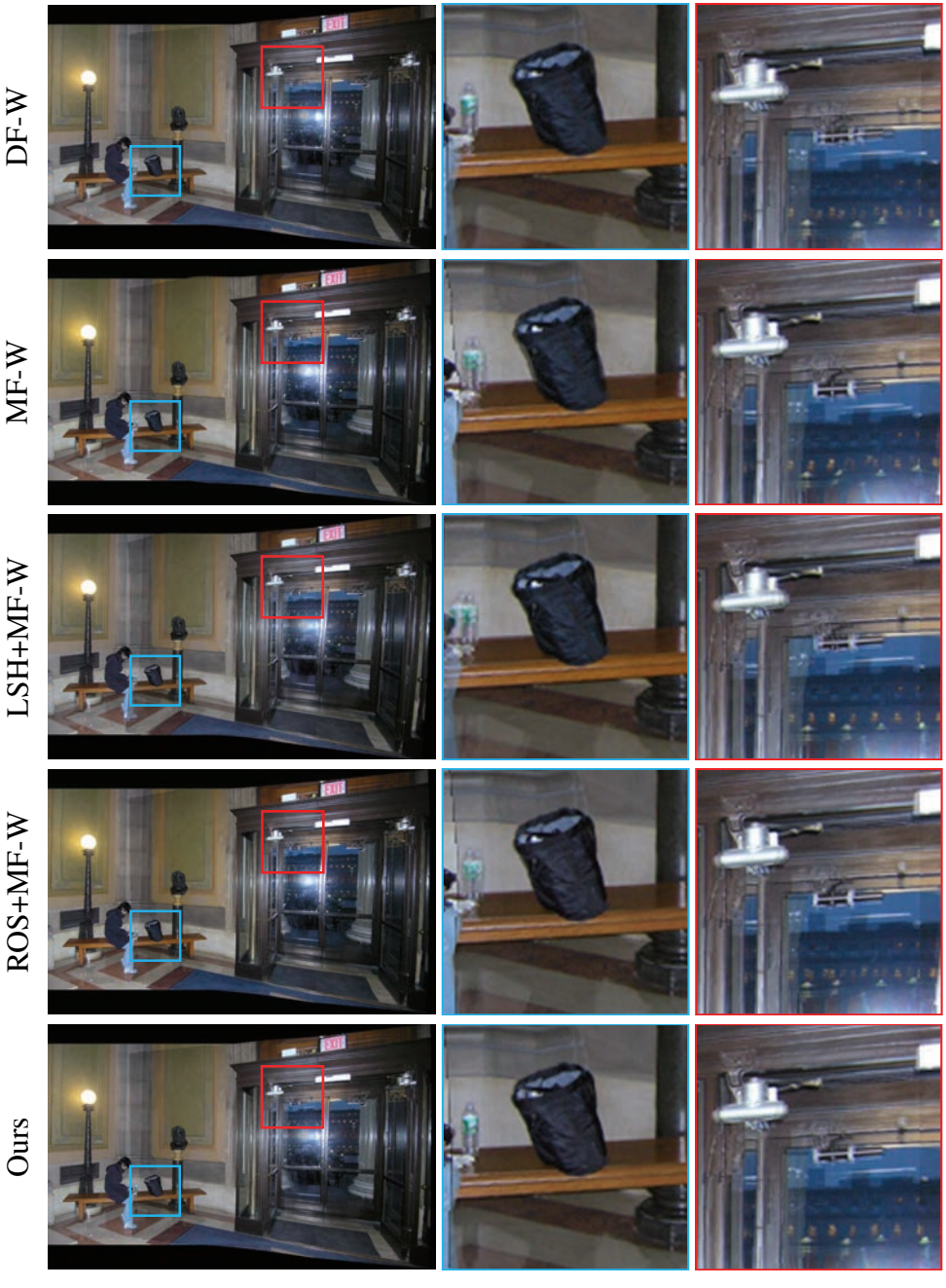

Figure 14: Comparisons with DF-W, MF-W, LSH+MF-W and ROS+MF-W: Image pair 05.

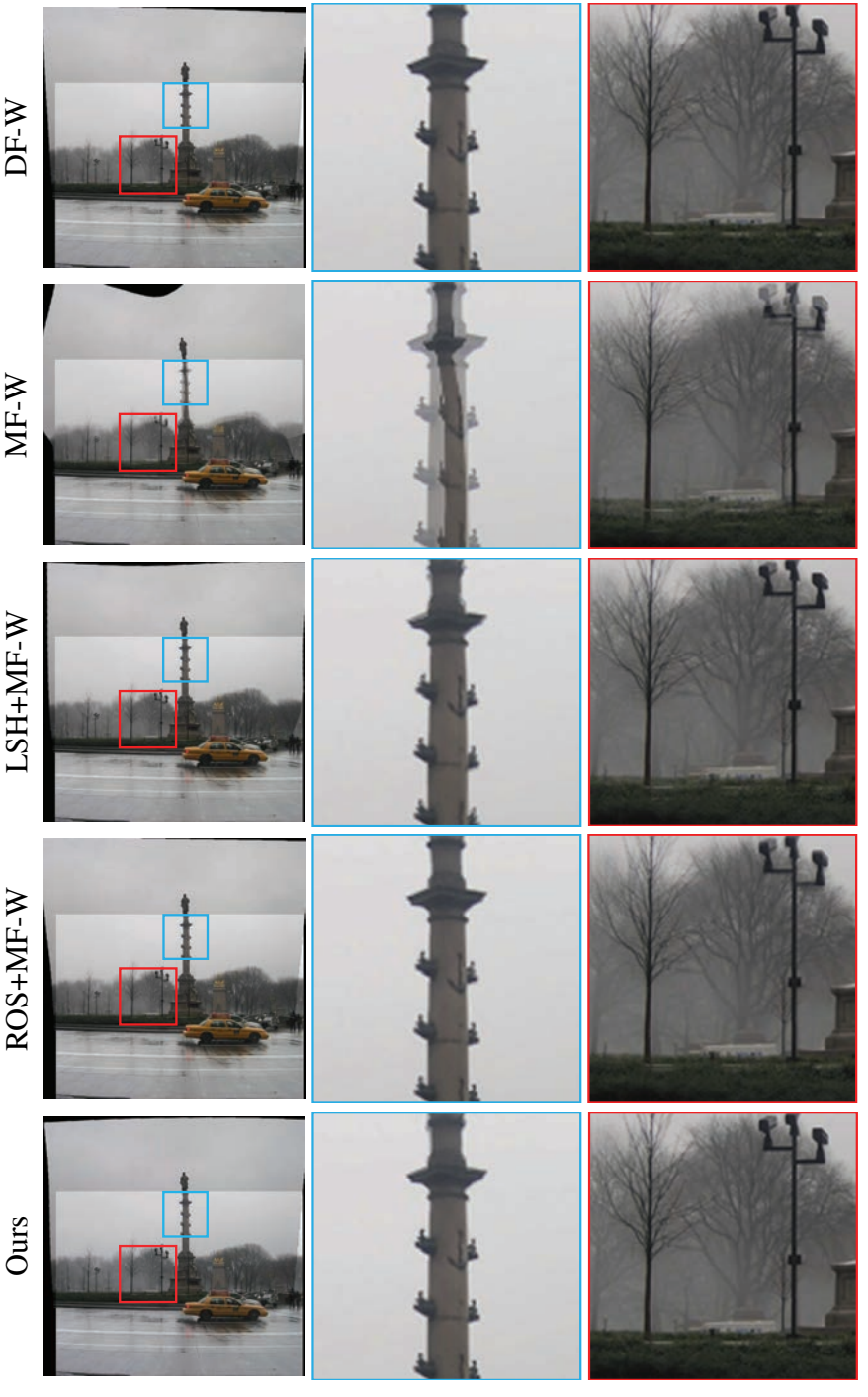

Figure 15: Comparisons with DF-W, MF-W, LSH+MF-W and ROS+MF-W: Image pair 06.

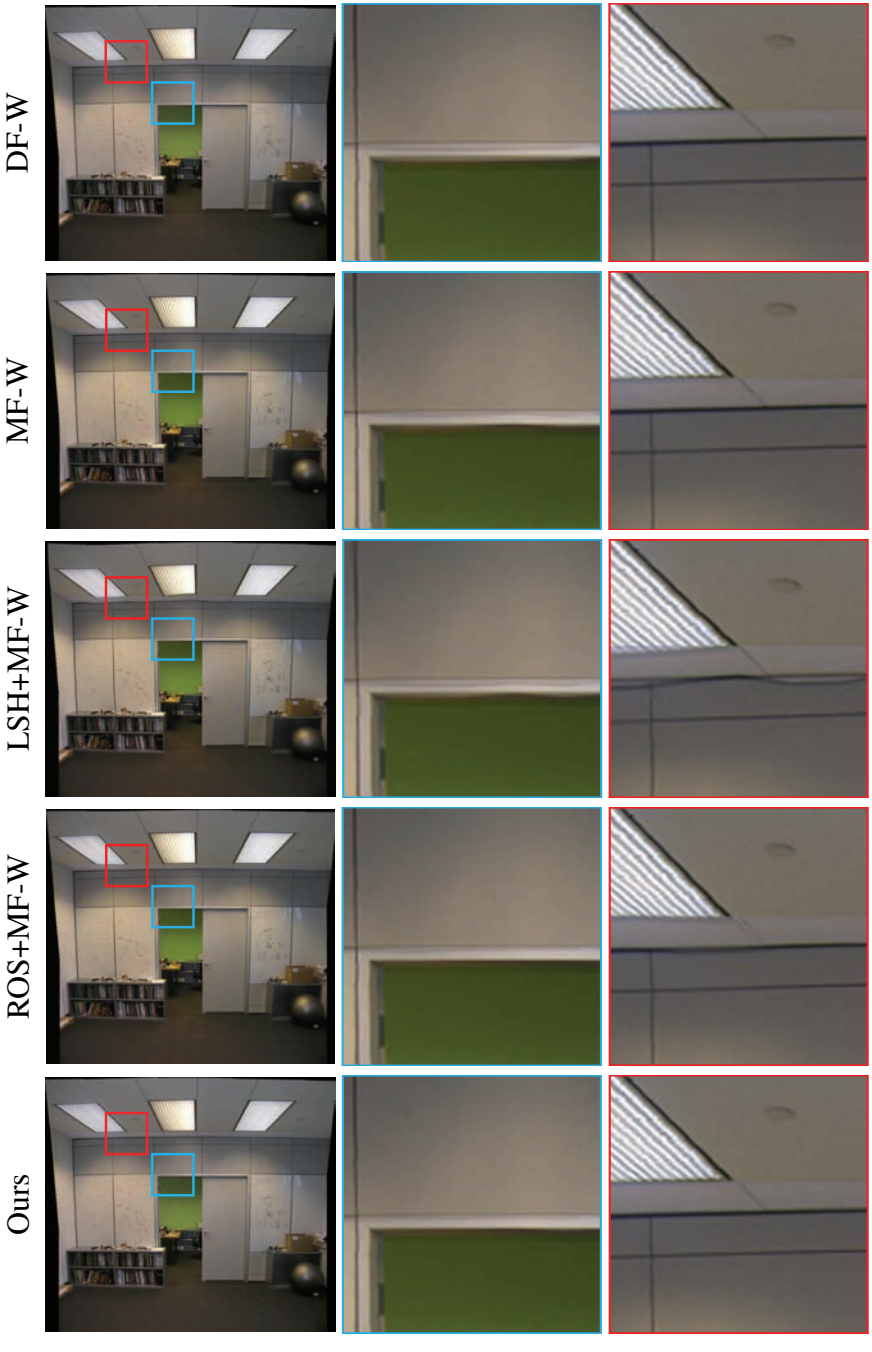

Figure 16: Comparisons with DF-W, MF-W, LSH+MF-W and ROS+MF-W: Image pair 07.

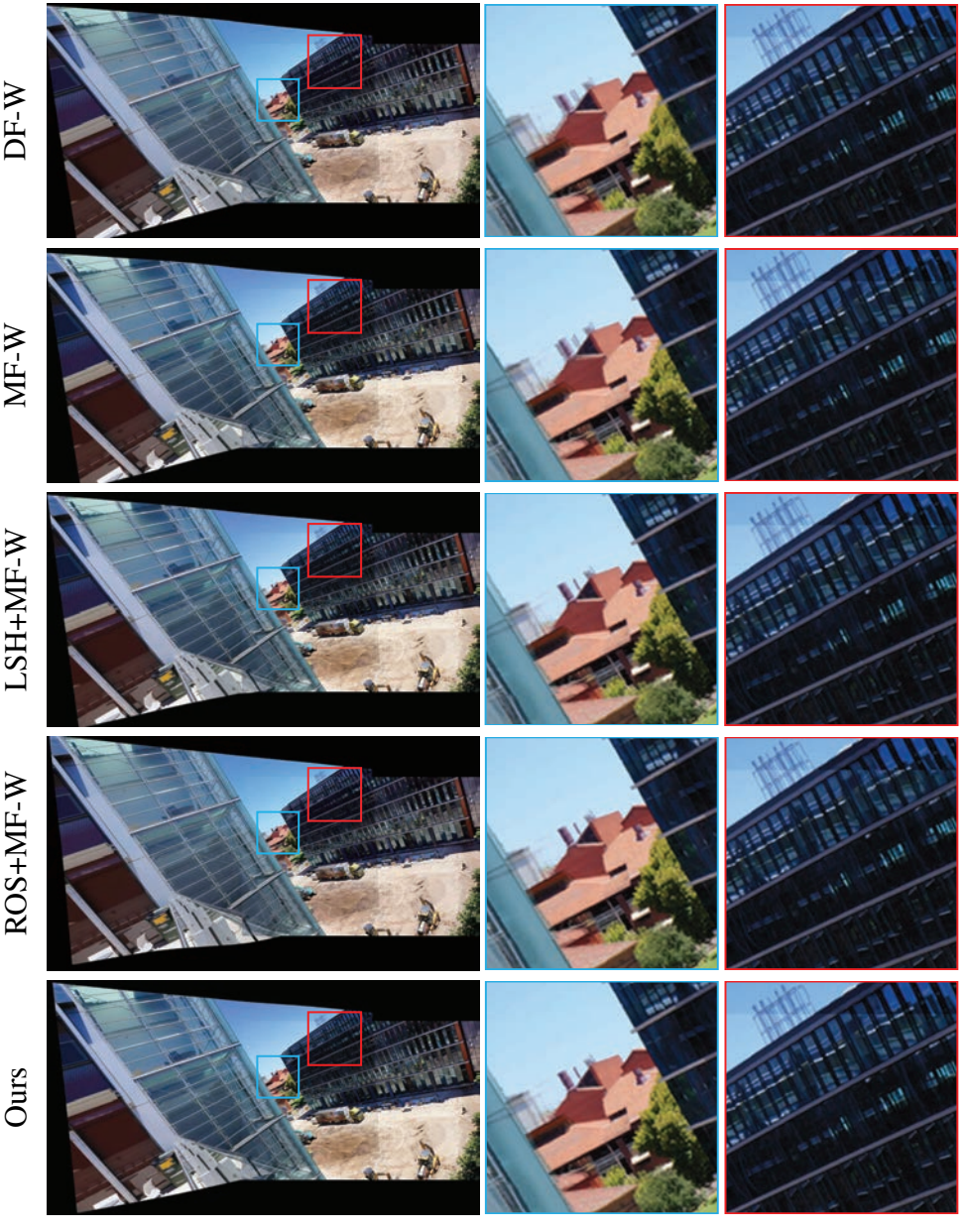

Figure 17: Comparisons with DF-W, MF-W, LSH+MF-W and ROS+MF-W: Image pair 08.

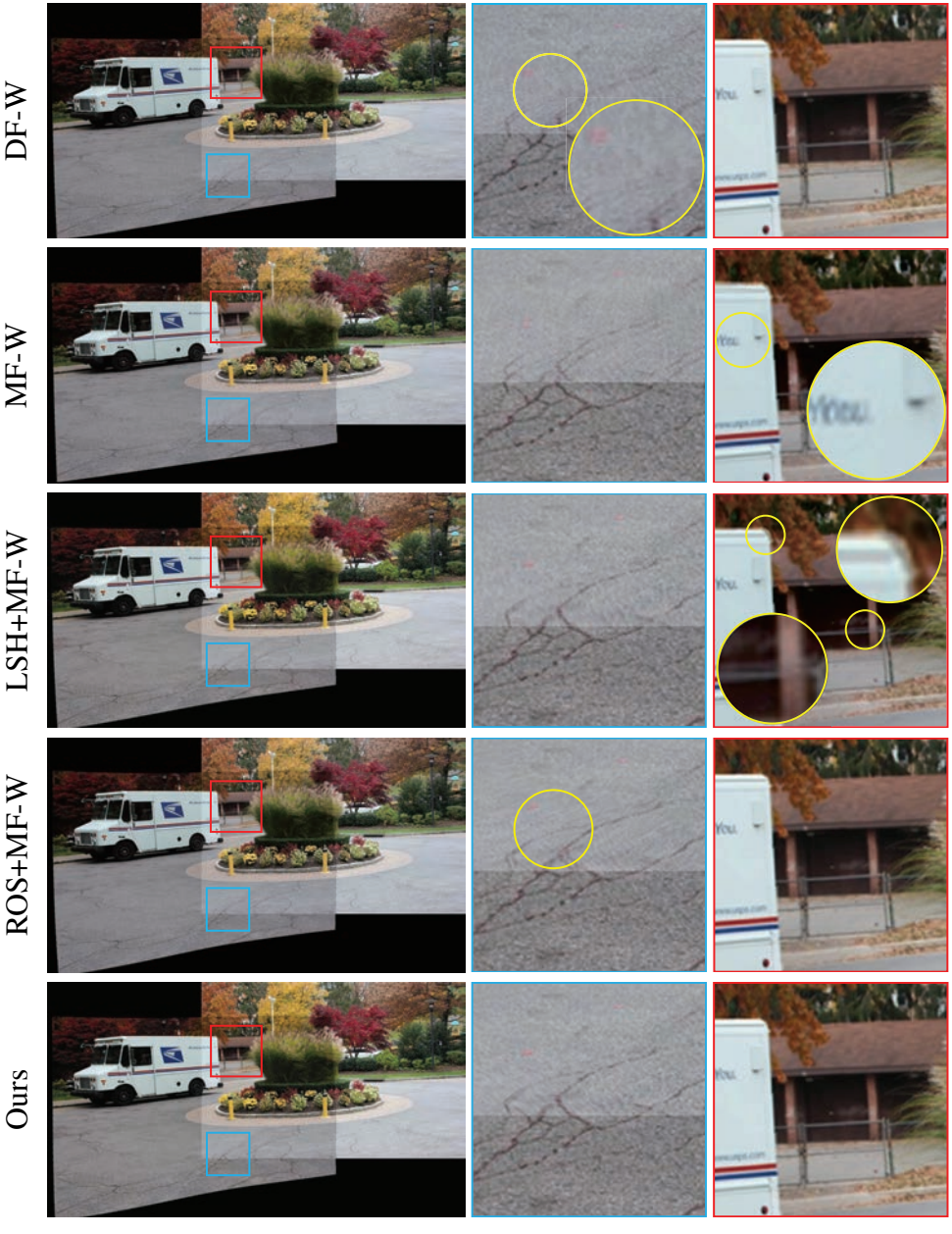

Figure 18: Comparisons with DF-W, MF-W, LSH+MF-W and ROS+MF-W: Image pair 09.

Figure 19: Comparisons with DF-W, MF-W, LSH+MF-W and ROS+MF-W: Image pair 10.